Physiologia Plantarum

ORIGINAL RESEARCH OPEN ACCESS

Adaptation of a Physiologically Based Model to Predict the Phenology of *Philaenus spumarius*, the Meadow Spittlebug

Zeinab Sweidan[1] | Oussama Bouaicha[2,3] | Nuray Baser[2] | Tito Caffi[1,4] | Stefania Gualano[2] | Vittorio Rossi[4] | Franco Santoro[2] | Marta Corbetta[1,5]

[1]Department of Sustainable Crop Production, Facoltà di Science Agrarie, Alimentari e Ambientali, Unviersità Cattolica del Sacro Cuore, Piacenza, Italy | [2]International Centre for Advanced Mediterranean Agronomic Studies of Bari (CIHEAM Bari), Valenzano, Italy | [3]Faculty of Agricultural, Environmental and Food Sciences, Free University of Bozen-Bolzano, Bolzano, Italy | [4]Research Centre on Plant Health Modelling, Università Cattolica del Sacro Cuore, Piacenza, Italy | [5]Horta srl, Piacenza, Italy

Correspondence: Tito Caffi (tito.caffi@unicatt.it)

Received: 27 August 2025 | **Revised:** 19 November 2025 | **Accepted:** 22 November 2025

Handling Editor: L. Rossini

Keywords: field data | model validation | olive agrosystems | *Philaenus spumarius* | physiologically-based model

ABSTRACT

The importance of *Philaenus spumarius* has grown considerably due to its role as a vector of *Xylella fastidiosa* (Xf), the bacterium responsible for olive quick decline syndrome (OQDS). Effective containment of Xf largely depends on vector management, including soil tillage to disrupt juvenile stages and timely insecticide applications to prevent adult spittlebugs from acquiring the bacterium from infected plants and becoming infectious. In this study, we adapted a physiologically based model to *P. spumarius*. As the pest is difficult to rear under laboratory conditions, we used field data from literature describing the temperature-dependent development of eggs, five juvenile stages (N1–N5), and adults across different crops and geographical areas. Development rate functions were developed from each literature source, and the most representative for the species were defined by adapting the Best Total Coverage method. The model was then validated using three independent datasets collected from different olive orchards across the Apulian region, Italy. The model showed good agreement between predicted and observed nymphal stages (N2 to N5), with R^2 values ranging from 0.829 to 0.960, depending on the orchard. However, the model showed a tendency to slightly anticipate the insect development. It also predicted the first seasonal emergence of adults with 88% accuracy. These findings demonstrate that field data can be effectively used to develop models for species that are difficult to rear under controlled conditions. The current model has strong potential to support monitoring and management programs by improving the timing of surveys, interventions, and control measures in olive orchards.

1 | Introduction

Plant diseases transmitted by vectors are known as vector-borne diseases. Understanding the phenology and ecology of vectors, such as arthropods, is essential for developing accurate models aimed at controlling both the vector and the disease. *Philaenus spumarius* L. (1758) (Hemiptera: Aphrophoridae), commonly known as the meadow spittlebug, is among the most polyphagous xylem-feeding pests (Thompson et al. 2023; Yurtsever 2000), and represents the primary vector of *Xylella fastidiosa* Wells et al. (1987) (Proteobacteria: Xanthomonadaceae, hereafter Xf) in Europe (Cornara et al. 2018, 2019). This bacterium represents one of the major threats to agriculture, as it affects economically important crops, including grapevine, citrus, olives, and stone fruits (Purcell 1997). It was first detected in Italy in 2013, with the Apulia region being particularly

affected (Saponari et al. 2013, 2019; Bodino et al. 2023). In the Salento peninsula alone, *X. fastidiosa* (Xf) has caused the loss of about 21 million olive trees with severe ecological and economic repercussions (Coldiretti 2023; Saponari et al. 2017). *X. fastidiosa* subsp. *pauca* was identified as the causal agent of the 'Olive quick decline syndrome' (OQDS) in the Apulia region (Scortichini 2022), and *P. spumarius* was confirmed to be the primary vector responsible for its spread (Cornara et al. 2017; Cavalieri et al. 2019). The outbreak of the OQDS has stimulated intense research on *P. spumarius* with particular attention to its biology, ecology, and control strategies (Cornara et al. 2018; Morelli et al. 2021).

The meadow spittlebug completes one generation per year (Witsack 1973; Cornara et al. 2018), overwintering in the egg stage that are laid in batches on herbs, or on herbaceous plants in autumn (Morente, Cornara, Moreno, et al. 2018; Weaver and King 1954), and typically hatch in early spring (Bodino et al. 2019, 2020). Nymphs pass through five nymphal instars (N1 to N5) over approximately 5 to 6 weeks, with early instars that often aggregate within the same spittle mass and are difficult to distinguish morphologically (Halkka et al. 1977; Bodino et al. 2020; Whittaker 1965; Fielding et al. 1999). However, late instar nymphs become more mobile, moving toward the plant apex, or crawling to nearby suitable host plants (Cornara et al. 2018). Adults begin mating shortly after emergence; however, females undergo ovarian parapause, which delays egg maturation. This physiological pause is regulated by the photoperiod and is accelerated as day length decreases (Morente et al. 2021). Consequently, egg maturation typically occurs at the end of summer, when mating activities increase (Cornara et al. 2018). Both juvenile and adult spittlebugs are xylem-sap feeders (Wiegert 1964; Malone et al. 1999); however, juveniles play a limited role in bacterial transmission, due to the loss of Xf transmission capacity after molting and to the low dispersal (Purcell and Finlay 1979).

Control strategies focus on monitoring vector presence and abundance, reducing nymphs, and preventing adult contact with olive trees (Morelli et al. 2021), mainly through timely interventions against juveniles and newly emerged adults, which in turn will limit the spread of Xf. Also, targeting the N4 peak is very effective in limiting its spread (Saponari et al. 2017; Cornara et al. 2018; Bodino et al. 2019; Morelli et al. 2021). Early stage monitoring (N1–N2) relies on visual inspections, which are complex, time-consuming, and require skilled personnel (Morelli et al. 2021), whereas adults are monitored using sweep nets on olive trees, as they migrate from herbaceous vegetation to arboreal hosts (Morente, Cornara, Plaza, et al. 2018).

Developing a phenological model that simulates the life cycle of *P. spumarius* can improve both pest monitoring and control strategies. Such models have been widely used to understand the population dynamics of *P. spumarius* in relation to environmental factors, primarily temperature. Typically, this is achieved by estimating the upper and lower developmental thresholds for nymphal stages or by using growing degree days (GDDs) accumulation to empirically describe the species' phenology (Chmiel and Wilson 1979a, 1979b; Zajac et al. 1989; Bodino et al. 2019; Beal et al. 2021).

A physiologically based demographic model (PBDM) initially developed by Gilioli et al. (2016) was recently adapted to *P. spumarius* (Gilioli et al. 2024) using development rate functions derived from laboratory rearing under constant temperature conditions. The continuous rearing of *P. spumarius* under controlled conditions remains challenging due to an incomplete understanding of the specific combination of environmental factors required (Cornara et al. 2018). This limitation can affect the reliability of quantitative data obtained under laboratory conditions. Therefore, Gilioli et al. (2024) calibrated the developmental rate functions using laboratory data in conjunction with field data collected from specific olive-growing areas. Through this calibration, the authors adjusted both the parameters of the development rate functions and the rule governing egg diapause termination, using weekly counts of nymphal stages N3, N4, and N5 for which more reliable monitoring data were available, as well as information on the first appearance of adults at the observed sites. This calibration led to significant changes in the function parameters and produced a plausible phenological dynamic when compared with independent observations collected in similar contexts. This type of calibration remains anchored to specific areas and years, which may limit the model's robustness when applied to different sites and years, thus requiring local recalibrations to ensure reliable outputs.

In this study, we parameterised the PBDM model developed by Gilioli et al. (2016) using field data retrieved from the literature on different *P. spumarius* populations. These data were used to develop population-specific developmental rate functions. Afterwards, we selected the functions of the population that most likely represent the species by adapting the Best Total Coverage (BTC) method, a criterion used by biologists to select representative model microorganisms to gain insights into biological processes of a taxon, for example a species or subspecies (Holland and Schmid 2005). Finally, we validated the model using the selected functions by running simulations against independent datasets collected across different sites and years.

2 | Materials and Methods

2.1 | Model Background

The PBDM, originally developed and validated for *Lobesia botrana* (Gilioli et al. 2016), was later adapted for *C. gnidiella* (Corbetta et al. 2025), *S. titanus* (Corbetta et al. 2024), and *P. spumarius* (Gilioli et al. 2024). It is based on a system of partial differential equations (Gardiner 1985) that describes the dynamics of a stage-structured insect population composed of i stages, where stages 1 to $s-1$ represent the immature stages, and stage s corresponds to the reproductive adult stage. A detailed description of the model's mathematical framework is provided in Gilioli et al. (2016). Here, we shortly introduce the main model equations:

$$\frac{\partial \emptyset^i}{\partial t} + \frac{\partial}{\partial x}\left[\upsilon^i(t)\emptyset^i - \sigma^i \frac{\partial \emptyset^i}{\partial x}\right] + m^i(t)\emptyset^i = 0, t > t_0, x \in (0,1) \quad (1)$$

$$\left[\upsilon^i(t)\emptyset^i\,(t,x) - \sigma^i \frac{\partial \emptyset^i}{\partial x}\right]_{x=0} = F^i(t) \quad (2)$$

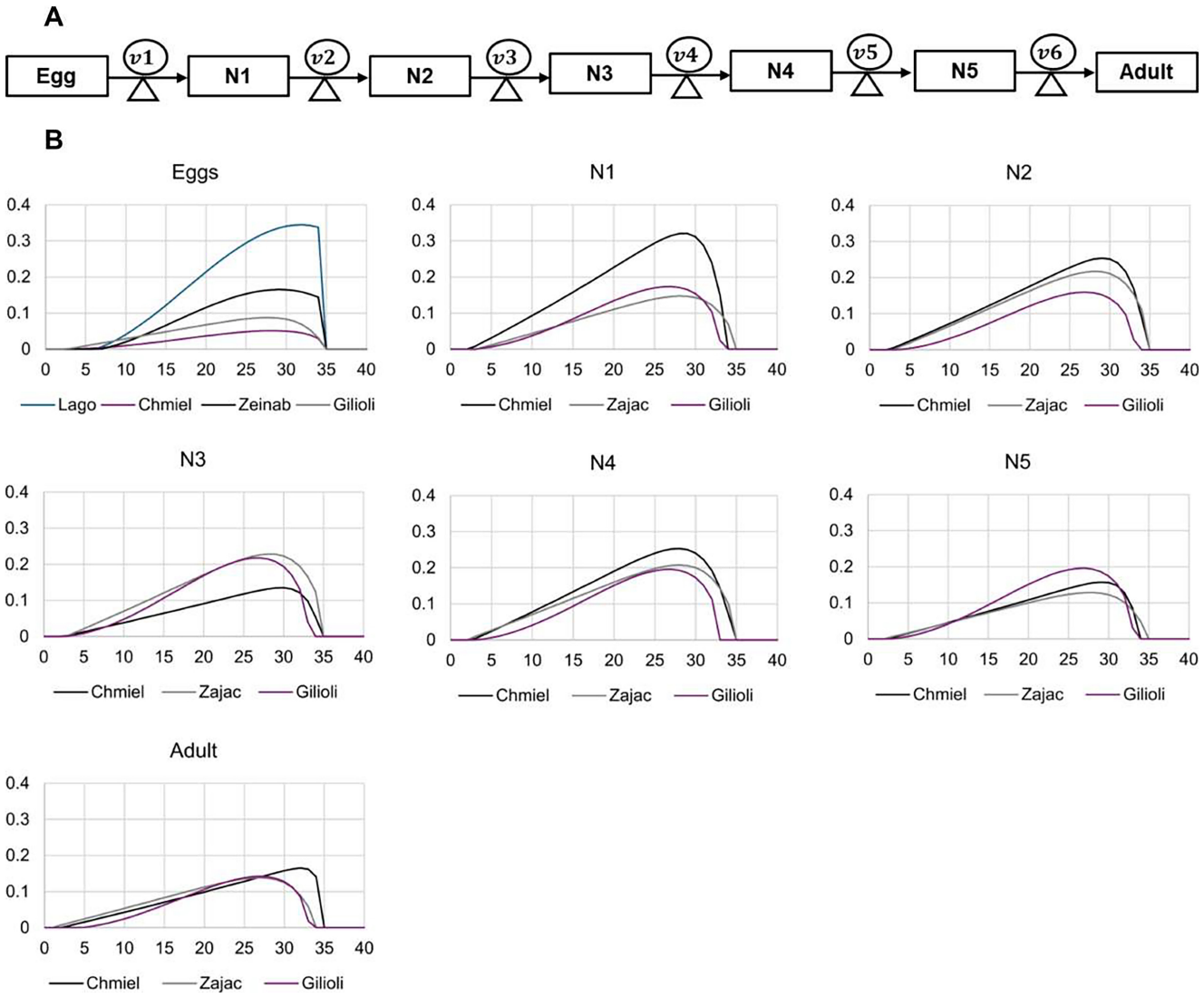

FIGURE 1 | (A) Simplified representation of the physiologically-based-demographic model for *Philaenus spumarius*. Developmental stages include eggs, five nymphal instars (N1–N5), and adults; υ1 to υ6 represent the temperature-dependent developmental rate functions for each stage. Mortality at any stage and adult fecundity, are not show, as these processes were not parameterised in the present model. The model simulates the phenological development of the insect population. (B) Temperature-dependent development rates for eggs, nymphal instars (N1 to N5), and adults of *Philaenus spumarius* based on data coming from different authors, fitted with the functions shown in Table S2.

$$\left[-\sigma^i \frac{\partial \emptyset^i}{\partial x}\right]_{x=1} = 0 \tag{3}$$

$$\emptyset^i\left(t_0, x\right) = \hat{\emptyset}^i(x) \tag{4}$$

where $i = 1, 2 \ldots, s$, represents the developmental stages of the insect; t is the chronological time; x represents the physiological age, that is, each individual's development over time; $\upsilon^i(t)$ and $m^i(t)$ are the stage specific development and mortality rates, respectively, which are assumed to be independent of physiological age x; $\emptyset^i(x)$ denotes the initial distribution of physiological age within a stage; σ^i is the diffusion coefficient, assumed as time-independent, which biologically represents the tendency to progress in physiological age (F^i being the flux of individuals). The function $\emptyset^i\left(t_0, x\right)$ provides the number of individuals in stage i at time t.

2.2 | Model Adaptation to *Philaenus spumarius*

Seven developmental stages of *P. spumarius* were considered (EPPO 2020): the egg stage ($i = 1$), five nymphal stages ($i = 2$–6), and the adult stage (s) (Figure 1A). *P. spumarius* is a univoltine species that overwinters in the egg stage (Cornara et al. 2018). Eggs are laid beginning around October, as observed by Cornara et al. (2018) under semi-controlled conditions. Other authors report that oviposition starts in September and continues until the death of the females (Barber and Ellis 1922; Weaver and King 1954; Yurtsever 2000). Weaver and King (1954) proved that eggs can hatch as early as February when exposed to temperatures below 15°C. Indeed, eggs overwinter until hatching occurs in early spring (Lago et al. 2023). In Pisa, eggs hatch in March, followed by juvenile development through five developmental stages during spring, with adult presence from late April or early May until November (Abenaim et al. 2025). In Apulia,

adult emergence typically occurs around late April and early May, with high population abundance observed from late spring to early summer, along with a noted movement from herbaceous plants to olive trees (EFSA 2019). However, as described in several studies, the timing of the life cycle may vary depending on environmental conditions (López Mercadal 2022).

2.2.1 | Development Functions

To parameterise the development rate functions of each life stage of *P. spumarius*, we used literature data. Specifically, the accumulated GDDs published by Chmiel and Wilson (1979a, 1979b), Zajac et al. (1989), and Lago et al. (2023), and the developmental rate functions calibrated by Gilioli et al. (2024). Additionally, an accumulation of 250 GDDs (base temperature 2.8°C) was considered for egg hatching, which roughly corresponds to the onset of the first seasonal nymphs in Apulia, based on our previous observations (Zeinab et al. unpublished).

Chmiel and Wilson (1979a) used laboratory and field data collected in 1977 near Greenhill, Indiana (US), to estimate the minimum temperature for egg development and the GDDs required for egg hatching. In a subsequent study, the same authors (1979b) estimated temperature thresholds and GDD-based durations for the nymphal and adult stages in alfalfa fields near Greenhill in 1978. Zajac et al. (1989) conducted a 2-year study in strawberry fields (at West Lafayette, Indiana, US, in 1983, and at Jeromesville, Ohio, US, in 1987) to estimate the first appearance, mean residence time, and duration of the nymphal and adult stages. Lago et al. (2023) monitored *P. spumarius* eggs from oviposition to hatching across four sites in the Iberian Peninsula in 2020, developing a GDD-based model for forecasting egg hatching. Gilioli et al. (2024) parametrised developmental rate functions for each life stage using laboratory data, which were later calibrated with field data collected in olive orchards in Liguria and Apulia, Italy (Bodino et al. 2019; Di Serio et al. 2019).

The GDD data derived from the above-mentioned sources are shown in Table S1. For eggs, GDDs represent the thermal time required for hatching based on a defined starting date for GDD accumulation (or biofix) and a minimum temperature threshold for development (T_{min}). Biologically, egg hatching coincides with diapause termination, a process that is difficult to detect (Lago et al. 2023). All these GDD methods assume that no development occurs below T_{min} during winter, and that diapause termination is linearly influenced by temperatures exceeding this base threshold (Chmiel and Wilson 1979a; Doherty et al. 2018; Kim et al. 2020). However, low winter temperatures may facilitate diapause termination, which then occurs once eggs are later exposed to warmer temperatures (Weaver and King 1954; Witsack 1973; Morente et al. 2021).

For any nymphal stage (N1–N5), the mean residence time (in GDDs) was calculated as the difference between the GDD_{50} of the current stage and that of the previous stage, where GDD_{50} denotes the midpoint of the stage (Zajac et al. 1989). For the adult stage, GDDs were measured from the emergence of the first adult until all nymphs had transitioned to the adults.

Data needed for fitting the development rate functions were obtained by converting GDDs for each stage into developmental rates following Gutierrez (1996): $(T_i - T_{min})/GDD$; where T_i is the average daily temperature on the ith day, and T_{min} is the developmental threshold of the corresponding stage. The GDDs related to egg hatching were extracted from Figure 3 of Lago et al. (2023) through digitization using GetData Graph Digitizer. To ensure accuracy, multiple replicates were performed, with relative deviations below 1%. The developmental rate function parameters from Gilioli et al. (2024) were extracted from the article, and the goodness-of-fit of the Brière function was evaluated based on these parameters.

The extracted developmental rate data were fitted to non-linear functions using the *nls* function from the "stats" package in R software (RStudio, version 2023.06.01). The best-fitting function was selected from several models commonly used to describe temperature-dependent insect development (Logan et al. 1976; Sharpe and DeMichele 1977; Bieri et al. 1983; Lactin et al. 1995; Briere et al. 1999), based on the Akaike Information Criterion (AIC) (Akaike 1981). Additionally, the coefficient of determination (R^2), root mean square error (RMSE), coefficient of residual mass (CRM), and concordance correlation coefficient (CCC) were calculated to evaluate goodness-of-fit, as shown in Table S2. Briefly, RMSE measures the average deviation between predicted and observed values, while CRM is a measure of the tendency of the equation to overestimate or underestimate the observed values (a negative CRM suggests overestimation) (Nash and Sutcliffe 1970). CCC is the product of the Pearson correlation coefficient and the coefficient C_b, which quantifies the difference between the best-fitting line and the line of perfect agreement (CCC = 1 means perfect agreement) (Madden et al. 2007). Resulting developmental curves are shown in Figure 1B.

To determine the equations to be used in adapting the PBDM to *P. spumarius*, we considered that the developmental data from each author represent the temperature response of a specific insect population. The main question, then, was how to choose the 'model population', that is, the population that best represents the developmental pattern of the species in response to temperature. To address this, we adapted the BTC approach, a criterion used by biologists to select representative model microorganisms to gain insights into biological processes of a given taxon, such as a species or subspecies (Holland and Schmid 2005). First, we calculated the distances, d, between pairs of insect populations for the developmental rates at any temperature level between 3°C and 43°C, using the functions listed in Table S2. Next, we defined $i = 17$ of T temperature thresholds for the d values (ranging from −0.2 to +0.2 in steps of 0.025), and set $d = 1$ if $d < T_i$, and $d = 0$ otherwise. We then plotted coverage curves for each population at the selected T thresholds; for instance, the coverage for $T = 0.05$ represents the percentage of the total d values within the interval ±0.05. The BTC method selects the population with the largest area beneath these curves as the most representative for the species (Holland and Schmid 2005). This approach enabled us to identify the population whose developmental rate function best captures the observed variability across several populations, ensuring that the model parameters are robust and representative for the species as a whole.

Additionally, we considered the distribution and statistics of the d values for each insect population. The best model population is

expected to have an average d close to zero, a narrow interquartile range, a low standard deviation, and a symmetric distribution (Holland and Schmid 2005).

2.2.2 | Mortality and Fecundity Functions

Limited information is available in the literature concerning the effects of environmental conditions on mortality and fecundity. Gilioli et al. (2023) evaluated adult mortality in the Apulia region at 0.015 individuals per day, based on the climatic conditions and data on adult emergence from the literature (Bodino et al. 2019; Di Serio et al. 2019).

Di Serio et al. (2019) evaluated the fecundity of *P. spumarius* using field-collected females maintained in small rearing cages in the Piedmont and Apulia regions. The females were kept on *Polygala mirtifolia* and *Medicago sativa* as host plants. Although females can lay up to 150 eggs, the average fecundity was approximately 90 and 20 eggs in Piedmont and Apulia, respectively, in 2017, and 113 and 18 eggs in 2018. However, these data are insufficient to develop a temperature-dependent fecundity function as required by the PBDM.

Because of these limitations, the demographic components of the model were not considered and both the mortality term $m^i(t)$ and the fertility flux $F^i(t)$ at the boundary conditions, $x=0$, were set to zero; therefore, the model simulates only the phenological development of the *P. spumarius* population. Specifically, the model provides, day by day, the distribution of individuals in each developmental stage, as represented in Figure 2.

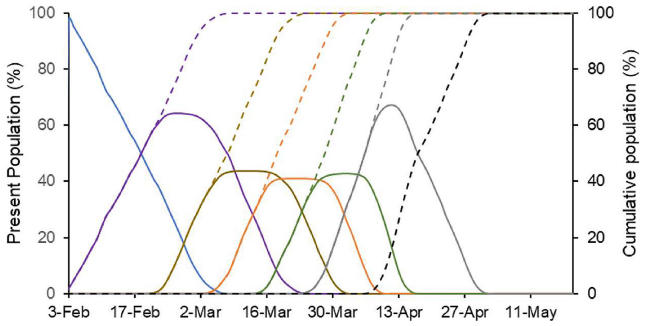

FIGURE 2 | Graphical output of the population dynamic of *Philaenus spumarius* as predicted by the PBDM. Both present (full line) and cumulative (dashed line) populations are shown in any day of the season, as a percentage of the total population of the day and as the percentage of individuals that have entered a stage, respectively. Colors indicate stages: Blue = eggs; violet = N1; brown = N2; orange = N3; green = N4; grey = N5; black = adults.

2.3 | Model Validation

Model validation was conducted using three independent datasets collected in the Apulia region. These datasets have been collected for monitoring the population dynamics of *P. spumarius* in olive orchards in relation to its role as a vector of Xf.

These datasets were collected following an official monitoring protocol (Puglia Region 2016). Briefly, nymphal stages were counted by randomly placing a 0.25 m^2 wooden frame on herbaceous vegetation; each foam and nymph within the frame was visually inspected and counted. Adult inspections were performed using an entomological net on olive trees (Di Serio et al. 2019).

The first dataset (hereinafter referred to as MAR19) was collected in 2019 from seven nearby olive orchards in Maruggio (Figure S1), along the Ionian coast of Taranto. Monitoring was performed biweekly in each orchard, recording individuals belonging to N1, N2 or N3, and N4 or N5 stages (i.e., no distinction was made between N2 and N3, or between N4 and N5). N1 individuals were recorded only occasionally and were excluded from model validation. Data collection continued until no more

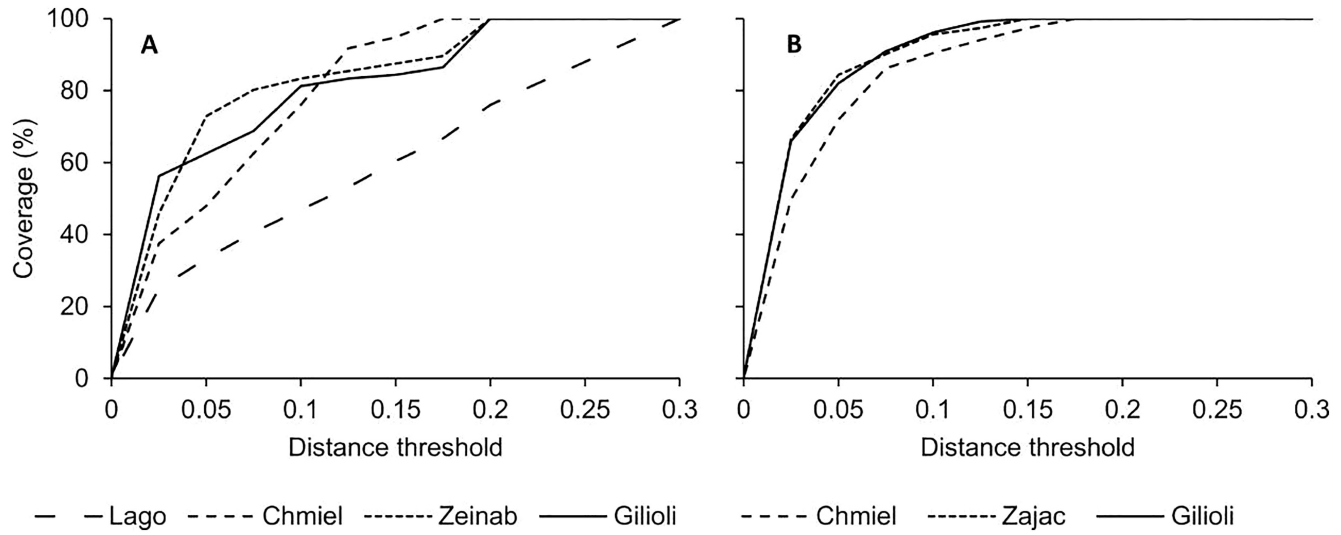

FIGURE 3 | Coverage plots developed based on the Best Total Coverage approach for describing the response to temperature for egg development (A) and for nymphal stages and adults (B) in different *Philaenus spumarius* populations (see Table S2). Distances (d) between the developmental rates at temperatures between 3°C and 34°C were calculated between pairs of populations, grouped at different threshold distances (between 0 and 0.3), and finally expressed as percentages; for instance, 50% coverage means that one half of the d values stay within ± the indicated distance threshold.

juvenile stages were observed; therefore, the duration of adult presence on the trees was not assessed. In preliminary analysis, the population development was uniform across the seven orchards; thus, the abundances of each developmental stage on each monitoring date were summed to represent the overall population in the area. The model was run using hourly temperature data from a single weather station (Pessl Instrument GmbH, Weiz, Austria) located approximately in a central position relative to the orchards (distances ranging from 0.21 to 0.85 km).

The second dataset (hereinafter EX24) was collected in 2024 from the regional cartographic service Emergenza Xylella (Emergenzaxylella.it 2024). Nine orchards in Bari and Taranto provinces were selected, each with at least four consecutive monitoring records (Figure S2 and Table S3); locations are identified by numbers (e.g., 16) as in the mentioned website. Monitoring was carried out at intervals ranging from a minimum of 8 days to a maximum of 17 days, with nymphal stages recorded separately from N1 to N5. Adults were counted until no more juveniles were observed. As with MAR19, N1 data were excluded because monitoring began too late to capture the whole N1 stage dynamic. The model was run for each orchard using hourly temperature data from the closest weather station (Pessl Instrument GmbH, Weiz, Austria), located within a maximum distance of 7.3 km.

The third dataset (hereinafter EX19) was set up with monitoring data from 41 olive orchards across the Apulia region (Southern Italy), in 2019, spanning altitudes from 8 to 436 m a.s.l. (monitoring site map in Anselmi 2022). Orchards were inspected on 25 March, 4 April, 12 April, 18 April, 30 April, 9 May, and 23 May. The proportion of the insect population in each developmental stage was determined, allowing identification of the first adult detection date. Temperature data for each site were obtained from the Horta weather station network (www.horta-srl.it) as described in Anselmi (2022).

Of these datasets, MAR19 and EX24 were used to compare observed (expressed as the number of individuals) and predicted (expressed as a percentage of the total population) nymphal stages. For each developmental stage, the cumulative number of individuals recorded across monitoring dates and orchards was expressed as a percentage of the total number of individuals observed in that stage throughout the entire monitoring period. For instance, at site 16 of EX24, the cumulative number of N3 at DOY (i.e., Day of the year) 87 was 4, while the total number of N3 at the end of monitoring was 14; therefore, the population at DOY 87 was 28.5% of the total (i.e., $4/14 \times 100$). The EX24 dataset was not used to validate the prediction of first adult onset due to variable and sometimes wide intervals between monitoring dates, reducing accuracy. Goodness-of-fit between predicted (P) and observed (O) data was evaluated using R^2 and the distribution of deviations, calculated as P−O.

The EX19 dataset was used to evaluate the model's ability to predict the presence of adults in orchards, a critical step for managing the *P. spumarius*—Xf system. Monitoring records were classified as either 1 or 0, based on whether there were adults or not, respectively. These data were analysed using a Receiver Operating Characteristic (ROC) curve, with model output for adults as the explanatory variable. The ROC curve plots the true positive proportion (TPP, or sensitivity, i.e., the proportion of positive records over total records) against the false negative proportion (FNP, or 1 − specificity, i.e., the proportion of negative records over total records) (Zweig and Campbell 1993; Hughes 2012). The overall explanatory ability of the model as a predictor of adult presence was expressed as the Area Under the ROC curve (AUROC) with a 95% confidence interval; the larger the AUROC (in the range from 0.5 to 1), the better the performance of the binary classifier system in distinguishing between the two groups (monitoring with or without adults). A *p*-value was calculated to test whether the AUROC was significantly different from the null hypothesis, that is, AUROC = 0.5 (the ROC curve coincides with the 1st diagonal, having 0,0 and 1,1 as coordinates), which indicates that the model is not able to distinguish between adult presence and absence. The ROC curve also helped define the optimal model output cut-off (Zweig and Campbell 1993) using the maximal value of the Youden index (J), that is, the vertical distance between any point on the ROC curve and the diagonal line, with 1 indicating a perfect test (Schisterman et al. 2005).

Posterior probabilities of correctly predicting adult presence or absence at this cut-off were calculated, and 2×2 contingency tables were prepared with cells containing the true positive proportion (TPP or sensitivity), true negative proportion (TNP or specificity), false positive proportion (FPP) and false negative proportion (FNP) (Madden et al. 2007). Each monitoring record, already classified for adults' presence (1) or absence (0), was reclassified based on whether the model output was below or above the cut-off (0 or 1, respectively). The posterior probabilities considered were: (1) adults found when predicted by the model cut-off, P(P+|O+) (thereinafter also referred as positive prediction); (2) no adults found when not predicted, P(P−|O−) (thereinafter also referred as negative prediction); (3) no adults found when predicted, P(P+|O−); and (iv) adults found when not predicted, P(P−|O+). These posterior probabilities were compared with prior probabilities of adults being sampled, calculated as the proportion of monitoring records with P(O+) or without P(O−) adults. Overall accuracy (OA) was calculated as the ratio of correct predictions to the total number of predictions. For incorrect predictions, the number of days between the predicted and actual adult presence was computed; shorter intervals indicate lower error.

3 | Results

3.1 | Model Adaptation

For model initialisation, it was assumed that the population consisted of 100% of individuals in the egg stage on the 1st of January. The physiological age $\emptyset^1(x)$ of these eggs was uniformly distributed over the interval [0, 1], representing a situation in which individuals had entered diapause at any point along the developmental continuum of the overwintering stage (Pasquali et al. 2019). This setting for the initial conditions better represents the data of Lago et al. (2023), who observed that eggs exposed to the same environmental conditions, at the same field site, hatched over a prolonged period, ranging from 34 to 43 days.

Concerning the developmental functions for eggs, the coverage curves showed some differences, with Lago and Zeinab representing the lowest and highest areas under the curve, respectively, while Chmiel had a lower area than both Zeinab and Gilioli (Figure 3A). The distribution of d values for the different insect populations showed an average d close to zero for Chmiel (0.004 ± 0.085), with Zeinab at $d = -0.047 \pm 0.091$, Gilioli at $d = -0.079 \pm 0.088$, and Lago at $d = 0.122 \pm 0.101$ (Figure 4A). Chmiel and Lago showed more symmetric data distributions, whereas Zeinab and Gilioli showed some negative skewness (−1.35 and −1.36, respectively) (Figure 4A). The distribution of distances among populations was strongly influenced by the Lago population, which showed unexpectedly higher egg developmental rates compared to the other populations (Figure 1B). Overall, the distribution of d values was similar for Zeinab and Gilioli. Notably, Gilioli's data were derived from Chmiel (since Gilioli et al. 2024, used the same biofix, T_{min} and GDDs to develop their function) but calibrated with field data (insect trapping) collected in Liguria (northern Italy) and Apulia (southern Italy), the latter being the same area where Zeinab calculated the GDDs for eggs. Based on the BTC approach and this consideration, the *P. spumarius* population identified by Zeinab was considered the most representative of the species and was therefore used in our PBDM for *P. spumarius* (see the row corresponding to the egg developmental stage in Table 1).

Concerning nymphal stages and adults, the coverage curve for Zajac and Gilioli was similar, with an area under the curve

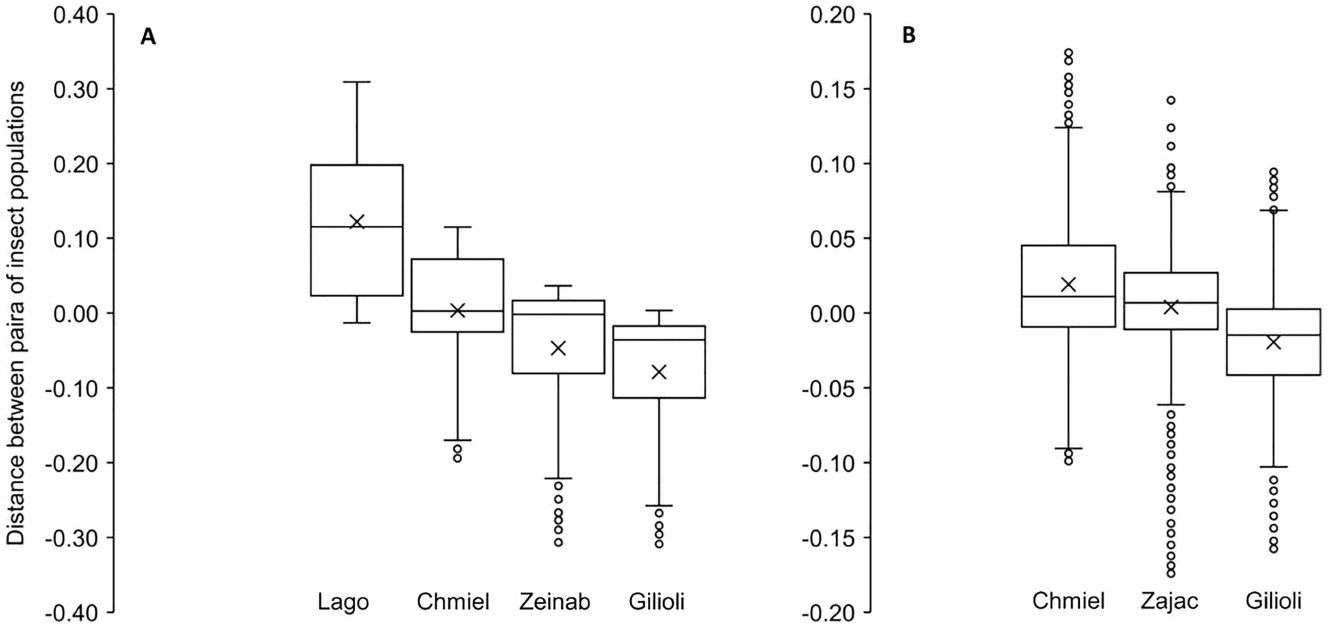

FIGURE 4 | Boxplots representing the distribution of the distances between the developmental rates for eggs (A) and for nymphal stages and adults (B) of different *Philaenus spumarius* populations (see Table S2), at temperatures between 3°C and 34°C. The boxes show the interquartile range, with the lower and upper ends corresponding to the 25th and 75th percentiles, respectively; the horizontal line within each box indicates the median (50th percentile), and the X marks the mean. Whiskers represent the range of the data, excluding outliers, which are displayed as individual points.

TABLE 1 | Estimated parameters of the Lactin functions and goodness-of-fit metrics for the developmental rate functions for *Philaenus spumarius* used in the model.

	Parameters				Goodness-of-fit			
Developmental stage	a	T_{max}	ΔT	γ	R^2	RMSE	CRM	CCC
Egg	0.0038	41.8	3.1	−1.00	0.999	0.0004	<0.0001	0.999
N1	0.0062	41.0	3.3	−1.01	0.997	0.0029	−0.0020	0.998
N2	0.0088	40.0	3.5	−1.03	0.999	0.0020	−0.0003	0.999
N3	0.0092	40.0	3.5	−1.04	0.999	0.0022	−0.0005	0.999
N4	0.0083	40.0	3.4	−1.02	0.999	0.0007	−0.0002	0.999
N5	0.0053	40.9	3.2	−1.01	1	0.0001	<0.0001	0.999
Adult	0.0056	40.7	3.1	−1.01	1	0.0001	<0.0001	0.999

Note: Goodness-of-fit was evaluated using the coefficient of determination (R^2), root mean square error (RMSE), coefficient of residual mass (CRM), and concordance correlation coefficient (CCC).

higher than that for Chmiel (Figure 3B). Zajac, however, had an overall (i.e., considering all nymphal stages and adults) average $d = 0.004 \pm 0.046$, which was closer to zero than Chmiel ($d = 0.019 \pm 0.056$) and Gilioli ($d = -0.019 \pm 0.047$), a narrower interquartile range (0.038 for Zajac, 0.054 for Chmiel, and 0.045 for Gilioli), and a more symmetric data distribution, with the average close to the median (Figure 4B). The developmental functions developed for the Zajac population were therefore considered the most representative of the species and were used in our PBDM for *P. spumarius* (see the rows corresponding to the N1–N5 nymphal stages and the adult stage in Table 1).

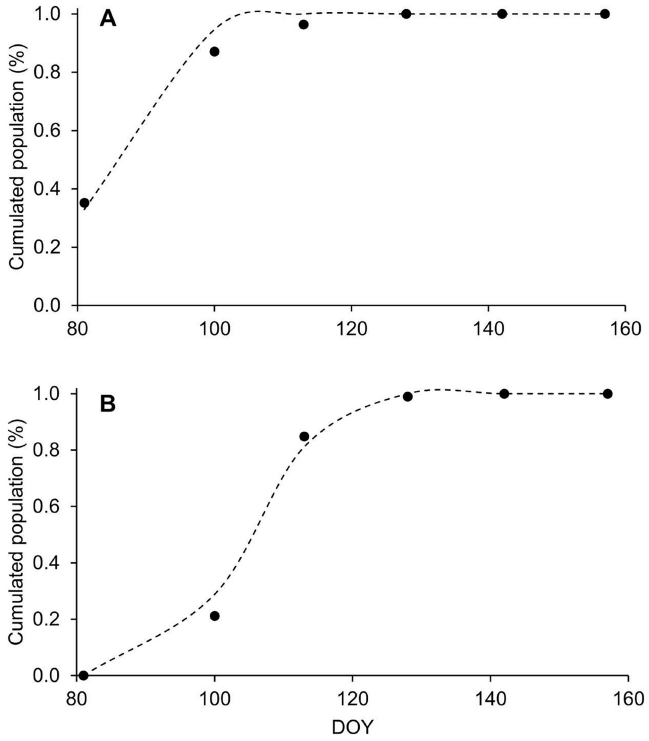

FIGURE 5 | Comparison between the predicted (dashed line) and observed (dots) development of *Philaenus spumarius* populations over time (expressed as DOY, Day of Year), for N2 + N3 (A) and N4 + N5 (B) nymphal stages in the MAR19 dataset.

3.2 | Model Validation

Figure 5 shows the relationship between the observed MAR19 data and the predicted populations of N2 + N3 (Figure 5A) and N4 + N5 (Figure 5B). The model showed good agreement with the observed data, with R^2 values of 0.976 for N2 + N3 and 0.993 for N4 + N5. The average deviation between predicted and observed populations was minimal, with values of 0.02 ± 0.02 for N2 + N3 and 0.01 ± 0.02 for N4 + N5, demonstrating the model's high accuracy in capturing the population dynamics for the MAR19 dataset.

Figure 6 compares predicted and observed data for each nymphal stage from N2 to N5 across different monitoring sites in EX24 (Figure 6A), as well as for all stages at each location (Figure 6B). The goodness-of-fit between the model and observed data increased progressively from N2 to N5, as demonstrated by increasing R^2 values, with the highest value (0.909) observed for N5 (Figure 6A). The model tended to accurately predict the observed populations, with an average deviation (P-O) ranging from 0.075 (with a 95% confidence interval of 0.050 to 0.125) for N1 to 0.115 (0.052 to 0.167) for N2 (Figure 6A). The fit at single locations was even better, with R^2 values ranging from 0.829 (L54) to 0.960 (L104) (Figure 6B). The model accurately predicted the observed data in 7 out of 9 locations (by an average of 0.111) and was slightly late in 2 locations (by an average of 0.015) (Figure 6B).

In the monitoring records of the EX19 dataset, the ROC analysis provided an $\text{AUROC} = 0.848 \pm 0.028$ ($p < 0.001$) for the presence of *P. spumarius* adults, indicating that the model is

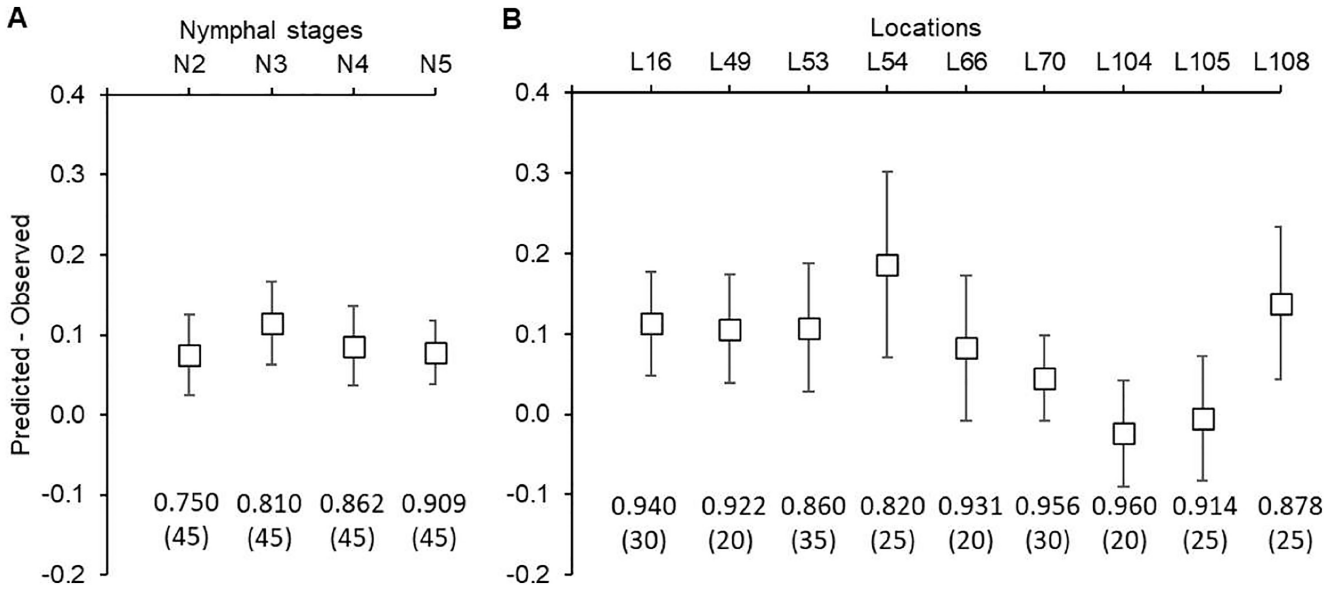

FIGURE 6 | Deviation of predicted (P) versus observed (O) populations of *Philaenus spumarius* nymphs for N2 to N5 (all locations) (A) and for single locations (all stages) (B) in the EX24 dataset. Dots show the average and whiskers the 95% confidence interval (i.e., the range that includes 95% of the data); numbers on the bottom show the R^2 of P versus O and the number of observations (between brackets).

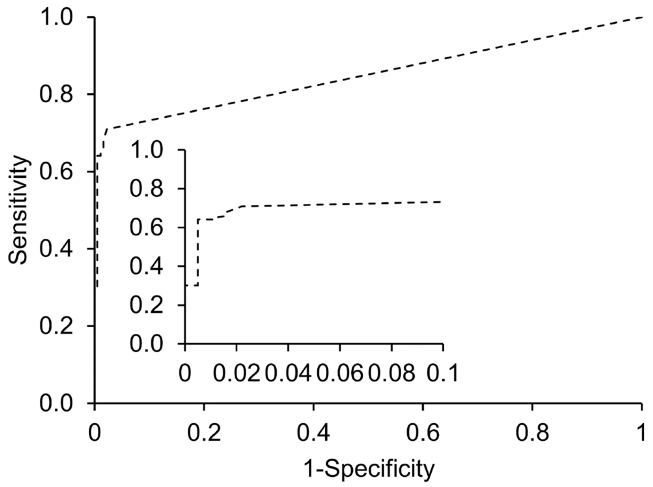

FIGURE 7 | Receiver operating characteristic (ROC) curve for using the PBDM output in predicting the presence of *Philaenus spumarius* adults in the EX19 dataset (consisting of 41 monitoring sites in 2019, in Apulia, Italy).

TABLE 2 | Contingency table showing the relationship between the observed and predicted presence or absence of *Philaenus spumarius* in the field, in 287 monitoring records from the EX19 dataset (consisting of 41 monitoring sites in 2019, in Apulia, Italy).

		Predicted		
		Yes	**No**	**Total**
Observed	Yes	73 TPP = 0.709	30 FNP = 0.291	103
	No	4 FPP = 0.022	180 TNP = 0.978	184
	Total	77	210	287
			Overall accuracy	0.882

Abbreviations: FNP, false negative proportion; FPP, false negative proportion; TNP, true negative proportion; TPP, true positive proportion.

a good binary classifier for distinguishing samplings with and without adults (Figure 7). The optimal model cut-off was estimated to be 0.000005 of accumulated adult proportion, providing an OA of 0.882, that is, > 88% of cases were correctly classified for the presence/absence of adults. Specifically, 253 out of 287 monitoring records were correctly classified, with TPP = 0.709 (sensitivity) and TNP = 0.978 (specificity) (Table 2). These results gave a posterior probability of positive samples P(P+|O+) = 0.948, which was 2.6 times higher than the prior probability of positive sampling P(O+) = 0.359. The posterior probability of correctly predicting adult absence P(P−|O−) was 0.860, also higher than the prior probability of negative sampling [P(O−)] = 0.641, confirming the utility of the model in predicting the presence of *P. spumarius* adults in orchards. The model also provided errors (in 34 cases out of 287), with P(P+|O−) = 0.052 for wrongly predicting adult presence, and P(P−|O+) = 0.140 for the model's failure to predict the presence of adults. In the 30 FN (i.e., false negative) cases, the model signaled adults' presence with an average delay of 7.4 days (with a 95% confidence interval of 5.5 to 9.2 days). In 3 out of 4 FP (i.e., false positive) cases, the model anticipated field observation of adults by 10 days (8.9 to 11.1 days), while in one case, no adults were observed during the monitoring period.

Similar results were obtained with the MAR19 dataset, where the model accurately predicted the onset of adult emergence without any delay. In fact, in MAR19, adults appeared on 23 April with a proportion of 0.015, which was accurately captured by the model, predicting a value of 0.022 for the adult stage on the same date.

4 | Discussion

Developing process-based phenological models, such as the one presented in this study, poses a key challenge: estimating model parameters that accurately reflect the biochemical and biophysical processes driving the transition between developmental stages in insects. These parameters are typically obtained from laboratory experiments conducted under controlled conditions, where individuals are regularly observed to collect quantitative data on species-specific traits. In such settings, both live and dead individuals are counted during each inspection, allowing researchers to track life-history traits such as development time, mortality, and fecundity under defined environmental conditions (Rossini et al. 2024). This type of experimental design has been widely used to evaluate how temperature affects the development, survival, and reproduction of insects (Régnière et al. 2012; Wang et al. 2009; Fiaboe et al. 2021; Baser et al. 2025). However, these studies are often expensive, time-consuming, and unfeasible for many species (Chuine and Jacques 2017). This is particularly true for *P. spumarius*, which is notoriously difficult to rear in laboratory conditions (Cornara et al. 2018). When laboratory experiments are impractical or may introduce uncertainties, field or semi-field observations, combined with meteorological data, provide a valuable and realistic alternative (Chuine and Jacques 2017).

In this study, we adapted a generic physiologically based demographic model (Gilioli et al. 2016) for *P. spumarius*, utilizing field-derived data from the literature. To represent the species' temperature-dependent development, we applied an adapted version of the BTC method (Holland and Schmid 2005). Although originally developed for selecting representative microorganisms, the BTC approach allowed us to account for intraspecific variability and to select a suitable representative population. Indeed, the studies listed in Table S1 examined *P. spumarius* populations collected from different locations and time periods. The variation observed in their developmental responses may reflect underlying genetic diversity within the species (Halkka et al. 1975; Seabra et al. 2021).

We validated the model using three independent datasets from Apulian olive orchards, across different sites, years, and conditions not used in the model development. Although these datasets were not specifically designed for validation, they provided a robust test of model reliability for three main reasons. First, their spatial and temporal heterogeneity (in sites, altitudes, years, and thermal regimes) expanded the range of tested

conditions, enhancing external validity under realistic and non-redundant conditions. Second, the chosen validation indicators (stage transition times, first adult emergence, and cumulative stage curves) were primarily driven by thermal accumulation and thus relatively insensitive to sampling irregularities (as in EX24) or missing absolute counts (as in EX19). Third, even without abundance data (as in EX19), proportional stage data anchored simulations to chronological events (e.g., instar peaks, first adults' appearance), enabling precise time deviation measurements and classification metrics (e.g., AUROC for adult presence/absence). Therefore, they provided a rigorous and realistic test for the model's robustness.

Validation results showed good agreement between predicted and observed data for nymphal stages N2 to N5, despite a slight tendency of the model to anticipate these stages. The ability to predict adult emergence timing with 88% accuracy is particularly relevant, since this marks the critical period for effective field interventions (Cornara et al. 2017). Upon emergence, adults migrate from herbaceous vegetation to olive trees, where they can acquire and transmit Xf (Cornara et al. 2017; Alma et al. 2019). The EX24 dataset, used to evaluate the model's ability to detect adult emergence, considered the first adult observed in the field, with monitoring activities conducted on both herbaceous and woody plants. Therefore, potential insect movement between vegetation types does not compromise the results. Moreover, targeting the N4 peak has proven to be effective in limiting the spread of *P. spumarius* (Saponari et al. 2017; Cornara et al. 2018; Bodino et al. 2019; Morelli et al. 2021). The good correlation between predicted and observed nymphal stages further supports the reliability of the model for informing this additional management strategy. Overall, these findings confirm that a reliable phenological model for a species that is difficult to rear under controlled conditions can be built, even in the absence of controlled rearing experiments. A previous study by Gilioli et al. (2024) employed the same mathematical framework as we did for *P. spumarius*. They initially developed developmental rate functions based on laboratory experiments, then calibrated them with field observations from olive orchards in Liguria and Apulia (Italy). While calibration improved accuracy, it also altered key function parameters, highlighting the uncertainty of controlled condition estimates for this species. Gilioli et al. (2024) finally validated the model using independent data collected from the same geographic areas, confirming improved accuracy following site-specific calibration. However, this approach may potentially limit the model's robustness when applied in different contexts or with different insect populations. Moreover, the absence of explicit evaluation metrics in Gilioli et al. (2024) prevents direct comparison with our model. It would therefore be valuable to compare the accuracy and robustness of the two calibration approaches, namely site-specific calibration and the use of representative field populations selected through the BTC method, by running both models on the same dataset using insect monitoring data collected across diverse regions and cropping systems where *P. spumarius* occurs and could play a role as Xf vector, such as vineyards and almond orchards (López-Mercadal et al. 2021).

It is important to emphasize that the existing models for *P. spumarius*, including the PBDM presented here, are still limited by gaps in current knowledge. Detailed data on egg diapause termination and its temporal distribution are still lacking, as well as information on the early nymphal stage (N1) and the adult stages. Addressing these gaps would significantly enhance the robustness and applicability of the model. Improved understanding of N1 onset could refine the timing of soil management strategies, such as those typically recommended in spring under the provisions of Determination No. 47/2025 (Comune di Monopoli 2025) issued by the Puglia Region. These practices aim to control the early nymphal stages of *P. spumarius* before the insects develop full flight capacity and disperse to new host plants. Similarly, improved knowledge of oviposition dynamics would support more targeted interventions while minimizing unnecessary soil disturbance.

In addition, although temperature is a key driver of insect development (Dangles et al. 2008; Liu et al. 2024), incorporating other environmental variables may be necessary to fully explain the variability observed in field populations of *P. spumarius*. Furthermore, the development of mortality and fecundity functions remains incomplete. Although Gilioli et al. (2023) estimated a constant adult mortality rate of 0.015 individuals per day, more detailed data are needed to develop temperature-dependent mortality functions. Moreover, as reported by Whittaker (1973) nymphal mortality is inversely density-dependent. However, mortality may also be influenced by additional factors, including the composition of herbaceous vegetation (Horsfield 1977) and the presence of predators and parasitoids (Molinatto et al. 2020; Benhadi-Marín et al. 2020). At its current stage, the model can support monitoring programs by helping to better schedule and organize surveys aimed at assessing the dynamics of *P. spumarius* populations in olive orchards, particularly in validated areas. It could also be integrated into decision support systems (DSS) for pest management, such as those recommended by Puglia Region (2016), that are based on adult emergence timing—a critical period that the model simulates with high accuracy.

Author Contributions

V.R., T.C., Z.S., M.C. conceived and designed the study. V.R., Z.S., M.C., O.B., N.B., S.G. and F.S. conducted the experiment and/or analysed the data. V.R., Z.S. and M.C. wrote the original draft. All the authors revised the manuscript and approved its final version.

Acknowledgments

Zeinab Sweidan conducted this study for the PhD in Agro-Food System (Agrisystem) at Università Cattolica del Sacro Cuore (Italy), cycle 38, scholarship no. 2360, I.3.3 PNRR, co-funded by Horta srl, and by the Portus project funded by the Romeo and Enrica Invernizzi Foundation. We gratefully acknowledge Horta srl for providing access to the framework used for running the model. This research was co-funded by the National Operational Program of the Italian Ministry of Education, University and Research (PON-MIUR) "AGREED-Agriculture, Green & Digital" ARS01_00254, Decreto concessione prot. n.580/2020, CUP. B94I200000170005, RNA-COR 1739311. Part of the dataset reported here was produced by CIHEAM Bari as part of the Master of Science in Innovative Approaches to Integrated Management of Mediterranean Fruit and Vegetable Crops.

Funding

The work was supported by the Horta srl, and by the Portus project funded by the Romeo and Enrica Invernizzi Foundation; National

Operational Program of the Italian Ministry of Education, University and Research (PON-MIUR).

Data Availability Statement

The data that support the findings of this study are available from the corresponding author upon reasonable request.

References

Abenaim, L., P. Farina, A. Mandoli, G. Conte, and B. Conti. 2025. *Biology and Integrated Control of Philaenus spumarius (Hemiptera: Aphrophoridae)*. Università di Pisa. https://hdl.handle.net/11568/1315087.

Akaike, H. 1981. "Likelihood of a Model and Information Criteria." *Journal of Econometrics* 16: 3–14. https://doi.org/10.1016/0304-4076(81)90071-3.

Alma, A., F. Lessio, and H. Nickel. 2019. "Insects as Phytoplasma Vectors: Ecological and Epidemiological Aspects." In *Phytoplasmas: Plant Pathogenic Bacteria-II: Transmission and Management of Phytoplasma-Associated Diseases*, 1–25. Springer Singapore.

Anselmi, A. 2022. "Un sistema di monitoraggio e di supporto alle decisioni per la gestione sostenibile dell'oliveto." PhD thesis, Università Cattolica del Sacro Cuore, Piacenza, Italy. https://publicatt.unicatt.it/retrieve/cb77bd95-237f-4b1b-b2ec-4c798006b959/Tesi%20PhD_Anselmi%20Andrea%20%2008-10-22.pdf.

Barber, G., and W. O. Ellis. 1922. "Eggs of Three Cercopidae." *Psyche (Stuttgart)* 29: 1–3.

Baser, N., L. Rossini, G. Anfora, et al. 2025. "Thermal Development, Mortality, and Fertility of an Apulian Strain of *Drosophila suzukii* at Different Temperatures." *Insects* 16, no. 1: 60.

Beal, D. J., M. Cooper, M. P. Daugherty, A. H. Purcell, and R. P. P. Almeida. 2021. "Seasonal Abundance and Infectivity of *Philaenus spumarius* (Hemiptera: Aphrophoridae), a Vector of *Xylella fastidiosa* in California Vineyards." *Environmental Entomology* 50, no. 2: 467–476.

Benhadi-Marín, J., M. Villa, L. F. Pereira, et al. 2020. "A Guild-Based Protocol to Target Potential Natural Enemies of *Philaenus spumarius* (Hemiptera: Aphrophoridae), a Vector of *Xylella fastidiosa* (Xanthomonadaceae): A Case Study With Spiders in the Olive Grove." *Insects* 11, no. 3: 100. https://doi.org/10.3390/insects11020100.

Bieri, M., J. Baumgartner, G. Bianchi, V. Delucchi, and R. Von. Arx. 1983. "Development and Fecundity of Pea Aphid (*Acyrthosiphon pisum* Harris) as Affected by Constant Temperatures and by Pea Varieties." *Mitteilungen der Schweizerischen Entomologischen Gesellschaft* 56: 163–171.

Bodino, N., V. Cavalieri, C. Dongiovanni, et al. 2019. "Phenology, Seasonal Abundance and Stage-Structure of Spittlebug (Hemiptera: Aphrophoridae) Populations in Olive Groves in Italy." *Scientific Reports* 9, no. 1: 1–17.

Bodino, N., V. Cavalieri, C. Dongiovanni, et al. 2020. "Spittlebugs of Mediterranean Olive Groves: Host-Plant Exploitation Throughout the Year." *Insects* 11, no. 2: 130.

Bodino, N., V. Cavalieri, C. DonGiovanni, M. Saponari, and D. Bosco. 2023. "Bioecological Traits of Spittlebugs and Their Implications on the Epidemiology and Control of *Xylella fastidiosa* Epidemic in Apulia (Southern Italy)." *Phytopathology* 113, no. 9: 1647–1660.

Briere, J. F., P. Pracros, A. Y. le Roux, and S. Pierre. 1999. "A Novel Rate Model of Temperature-Dependent Development for Arthropods." *Environmental Entomology* 28: 22–29.

Cavalieri, V., G. Altamura, G. Fumarola, et al. 2019. "Transmission of *Xylella fastidiosa* Subspecies Pauca Sequence Type 53 by Different Insect Species." *Insects* 10, no. 10: 324. https://doi.org/10.3390/insects10100324.

Chmiel, S. M., and M. C. Wilson. 1979a. "Estimating Threshold Temperature and Heat Unit Accumulation Required for Meadow Spittlebug Egg Hatch." *Environmental Entomology* 8: 612–614.

Chmiel, S. M., and M. C. Wilson. 1979b. "Estimation of the Lower and Upper Developmental Threshold Temperatures and Duration of the Nymphal Stages of the Meadow Spittlebug, *Philaenus spumarius*." *Environmental Entomology* 8, no. 4: 682–6856.

Chuine, I., and R. Jacques. 2017. "Process-Based Models of Phenology for Plants and Animals." *Annual Review of Ecology, Evolution, and Systematics* 48: 159–182.

Coldiretti. 2023. "Xyella: Goodbye 21 Million Olive Trees. The Bacterium Advances 20 km a Year. Xylella Has Affected 40% of Puglia." https://www.retegargano.it/2023/05/01/coldiretti-addio-21-milioni-di-ulivi-il-batterio-avanza-20-km-allanno-la-xylella-ha-colpito-il-40-della-puglia/.

Comune di Monopoli. 2025. "Determination No. 47/2025." https://www.comune.monopoli.ba.it/Novita/Avvisi/Applicazione-delle-misure-fitosanitarie-di-lotta-al-vettore-per-il-contrasto-ed-il-controllo-di-Xylella-fastidiosa#:~:text=Sulla%20base%20dell'attuale%20andamento,sino%20al%2030%20aprile%202025.

Corbetta, M., G. Benelli, R. Ricciardi, V. Rossi, and A. Lucchi. 2025. "Adaptation of a Physiologically Based Demographic Model for Predicting the Phenology of *Cryptoblabes gnidiella* With Validation in Italian Vineyards." *Journal of Pest Science* 98: 929–942.

Corbetta, M., S. Legler, S. Lioy, and V. Rossi. 2024. "Validation of a Physiologically Based Demographic Model for Scaphoideus Titanus Ball (Fam. Cicadellidae)." *IOBC-WPRS Bulletin Working Group Integrated Protection in Viticulture* 171: 18–23.

Cornara, D., D. Bosco, and A. Fereres. 2018. "*Philaenus spumarius*: When an Old Acquaintance Becomes a New Threat to European Agriculture." *Journal of Pest Science* 91: 957–972.

Cornara, D., M. Morente, A. Markheiser, et al. 2019. "An Overview on the Worldwide Vectors of *Xylella fastidiosa*." *Entomologia Generalis* 39, no. 3–4: 157–181.

Cornara, D., M. Saponari, A. R. Zeilinger, et al. 2017. "Spittlebugs as Vectors of *Xylella fastidiosa* in Olive Orchards in Italy." *Journal of Pest Science* 90, no. 2: 521–530.

Dangles, O., C. Carpio, A. R. Barragan, J. Zeddam, and J. Silvain. 2008. "Temperature as a Key Driver of Ecological Sorting Among Invasive Pest Species in the Tropical Andes." *Ecological Applications* 18: 1795–1809.

Di Serio, F., N. Bodino, V. Cavalieri, et al. 2019. "Collection of Data and Information on Biology and Control of Vectors of *Xylella fastidiosa*." *External Scientific Report* 16, no. 5: 1628E.

Doherty, J. F., J. F. Guay, and C. Cloutier. 2018. "Novel Temperature-Dependent Development Rate Models for Post Diapause Egg Eclosion of Three Important Arthropod Pests Found in Commercial Christmas Tree Plantations of Southern Québec, Canada." *Environmental Entomology* 47, no. 3: 715–724. https://doi.org/10.1093/ee/nvy003.

Emergenzaxylella.it. 2024. "Emergenza Xylella." http://emergenzaxylella.it/portal/portale_gestione_agricoltura.

EPPO. 2020. "PM 7/141 (1) – *Philaenus spumarius*, *Philaenus italosignus* and *Neophilaenus campestris*." https://gd.eppo.int/taxon/PHILSU/documents.

Fiaboe, K. K., S. Kekeunou, S. N. Nanga, et al. 2021. "Temperature-Based Phenology Model to Predict the Development, Survival, and Reproduction of the Oriental Fruit Fly *Bactrocera dorsalis*." *Journal of Thermal Biology* 97: 102877.

Fielding, C. A., J. B. Whittaker, J. E. L. Butterfield, and J. C. Coulson. 1999. "Predicting Responses to Climate Change: The Effect of Altitude and Latitude on the Phenology of the Spittlebug *Neophilaenus lineatus*." *Functional Ecology* 13, no. 1: 65–73.

Gardiner, C. W. 1985. *Handbook of Stochastic Methods*. Springer.

Gilioli, G., A. Simonetto, I. D. Weber, et al. 2024. "A Model for Predicting the Phenology of *Philaenus spumarius*." *Scientific Reports* 14: 8137.

Gilioli, G., A. Simonetto, M. G. Naso, et al. 2023. "An Eco-Epidemiological Model Supporting Rational Disease Management of *Xylella fastidiosa*. An Application to the Outbreak in Apulia (Italy)." *Ecological Modelling* 476: 110226.

Gilioli, G., S. Pasquali, and E. A. Marchesini. 2016. "Modelling Framework for Pest Population Dynamics and Management: An Application to the Grape Berry Moth." *Ecological Modelling* 320: 348–357.

Gutierrez, A. P. 1996. *Applied Population Ecology: A Supply-Demand Approach*. John Wiley & Sons.

Halkka, O., M. Raatikainen, and J. Vilbaste. 1975. "Clines in the Colour Polymorphism of *Philaenus spumarius* in Eastern Central Europe." *Heredity* 35: 303–309.

Halkka, O., M. Raatikainen, L. Halkka, and T. Raatikainen. 1977. "Coexistence of Four Species of Spittle Producing Homoptera." *Annales Zoologici Fennici* 14: 228–231.

Holland, B. R., and J. Schmid. 2005. "Selecting Representative Model Micro-Organisms." *BMC Microbiology* 5, no. 1: 26.

Horsfield, D. 1977. "Relationships Between Feeding of *Philaenus spumarius* (L.) and the Amino Acid Concentration in the Xylem Sap." *Ecological Entomology* 2: 259–266. https://doi.org/10.1111/j.1365-2311.1977.tb00889.x.

Hughes, G. 2012. *Applications of Information Theory to Epidemiology*. American Phytopathological Society.

Kim, M. J., S. Baek, and J. H. Lee. 2020. "Egg Hatching and First Instar Falling Models of *Metcalfa pruinosa* (Hemiptera: Flatidae)." *Insects* 11, no. 6: 345.

Lactin, D. J., N. J. Holliday, D. L. Johnson, and R. Craigen. 1995. "Improved Rate Model of Temperature-Dependent Development by Arthropods." *Environmental Entomology* 24, no. 1: 68–75.

Lago, C., A. Moreno, A. Giménez-Romero, M. Morente, and A. Fereres. 2023. "Degree-Day-Based Model to Predict Egg Hatching of *Philaenus spumarius* (Hemiptera: Aphrophoridae), the Main Vector of *Xylella fastidiosa* in Europe." *Environmental Entomology* 52: 1–10.

Liu, Z., B. Liu, H. Yu, H. Zhang, Z. He, and Z. Zhuo. 2024. "The Effects of Global Climate Warming on the Developmental Parameters of *Helicoverpa armigera* (Hübner, 1808) (Lepidoptera: Noctuidae)." *Insects* 15, no. 11: 888.

Logan, J. A., D. J. Wollkind, S. C. Hoyt, and L. K. Tanigoshi. 1976. "An Analytic Model for Description of Temperature Dependent Rate Phenomena in Arthropods." *Environmental Entomology* 5, no. 6: 1133–1140.

López Mercadal, J. 2022. "Seasonality, Life Cycle and Vectorial Capacity of *Xylella fastidiosa* Insect Vectors in the Main Crops of the Balearic Islands." https://www.tdx.cat/handle/10803/675508.

López-Mercadal, J., S. Delgado, P. Mercadal, et al. 2021. *Collection of Data and Information in Balearic Islands on Biology of Vectors and Potential Vectors of Xylella fastidiosa (GP/EFSA/ALPHA/017/01)*, 136. EFSA Supporting Publication. https://doi.org/10.2903/sp.efsa.2021.EN-6925.

Madden, L. V., G. Hughes, and F. Van Den Bosch. 2007. *The Study of Plant Disease Epidemics*. American Phytopathological Society.

Malone, M., R. Watson, and J. Pritchard. 1999. "The Spittlebug *Philaenus spumarius* Feeds From Mature Xylem at the Full Hydraulic Tension of the Transpiration Stream." *New Phytologist* 143, no. 2: 261–271.

Molinatto, G., S. Demichelis, N. Bodino, M. Giorgini, N. Mori, and D. Bosco. 2020. "Biology and Prevalence in Northern Italy of *Verrallia aucta* (Diptera, Pipunculidae), a Parasitoid of *Philaenus spumarius* (Hemiptera, Aphrophoridae), the Main Vector of *Xylella fastidiosa* in Europe." *Insects* 11, no. 9: 607. https://doi.org/10.3390/insects11090607.

Morelli, M., J. M. García-Madero, Á. Jos, et al. 2021. "*Xylella fastidiosa* in Olive: A Review of Control Attempts and Current Management." *Microorganisms* 9, no. 8: 1771.

Morente, M., D. Cornara, A. Moreno, and A. Fereres. 2018. "Continuous Indoor Rearing of Philaenus Spumarius, the Main European Vector of Xylella Fastidiosa." *Journal of Applied Entomology* 142, no. 9: 901–904.

Morente, M., D. Cornara, A. Moreno, and A. Fereres. 2021. "Parapause Breakage as a Key Step for the Continuous Indoor Rearing of *Philaenus spumarius*." *Journal of Applied Entomology* 145, no. 10: 1062–1067.

Morente, M., D. Cornara, M. Plaza, et al. 2018. "Distribution and Relative Abundance of Insect Vectors of *Xylella fastidiosa* in Olive Groves of the Iberian Peninsula." *Insects* 9, no. 4: 175.

Nash, J. E., and J. V. Sutcliffe. 1970. "River Flow Forecasting Through Conceptual Models Part I — A Discussion of Principles." *Journal of Hydrology* 10, no. 3: 282–290.

Pasquali, S., S. Cinzia, and G. Gilioli. 2019. "The Effects of Fecundity, Mortality and Distribution of the Initial Condition in Phenological Models." *Ecological Modelling* 402: 45–58.

Puglia Region. 2016. "Deliberazione della Giunta Regionale n. 1708/2016: Approvazione del protocollo di monitoraggio ufficiale." https://cartografia.sit.puglia.it/doc/xylella/1999.pdf.

Purcell, A. H. 1997. "*Xylella fastidiosa*, a Regional Problem or Global Threat." *Journal of Plant Pathology* 79: 99–105.

Purcell, A. H., and A. H. Finlay. 1979. "Evidence for Noncirculative Transmission of Pierce's Disease Bacterium by Sharpshooter Leafhoppers." *Phytopathology* 69: 393–395.

Régnière, J., J. Powell, B. Bentz, and V. Nealis. 2012. "Effects of Temperature on Development, Survival and Reproduction of Insects: Experimental Design, Data Analysis and Modeling." *Journal of Insect Physiology* 58, no. 5: 634–647. https://doi.org/10.1016/j.jinsphys.2012.01.010.

Rossini, L., M. Contarini, S. Speranza, et al. 2024. "Life Tables in Entomology: A Discussion on Tables' Parameters and the Importance of Raw Data." *PLoS One* 19, no. 3: e0299598.

Saponari, M., A. Giampetruzzi, G. Loconso le, D. Boscia, and P. Saldarelli. 2019. "Xylella Fastidiosa in Olive in Apulia: Where We Stand." *Phytopathology* 109: 175–186.

Saponari, M., D. Boscia, F. Nigro, and G. P. Martelli. 2013. "Identification of DNA Sequences Related to *Xylella fastidiosa* in Oleander, Almond and Olive Trees Exhibiting Leaf Scorch Symptoms in Apulia (Southern Italy)." *Journal of Plant Pathology* 95, no. 3: 668.

Saponari, M., D. Boscia, G. Altamura, et al. 2017. "Isolation and Pathogenicity of *Xylella fastidiosa* Associated to the Olive Quick Decline Syndrome in Southern Italy." *Scientific Reports* 7: 17723.

Schisterman, E. F., N. J. Perkins, A. Liu, and H. Bondell. 2005. "Optimal Cut-Point and Its Corresponding Youden Index to Discriminate Individuals Using Pooled Blood Samples." *Epidemiology* 16: 73–81.

Scortichini, M. 2022. "The Epidemiology and Control of "Olive Quick Decline Syndrome" in Salento (Apulia, Italy)." *Agronomy* 12, no. 10: 2475.

Seabra, S. G., A. S. B. Rodrigues, S. E. Silva, et al. 2021. "Population Structure, Adaptation and Divergence of the Meadow Spittlebug, *Philaenus spumarius* (Hemiptera, Aphrophoridae), Revealed by Genomic and Morphological Data." *PeerJ* 9: e11425.

Sharpe, P. J., and D. W. DeMichele. 1977. "Reaction Kinetics of Poikilotherm Development." *Journal of Theoretical Biology* 64, no. 4: 649–670.

Thompson, V., C. Harkin, and A. J. A. Stewart. 2023. "The Most Polyphagous Insect Herbivore? Host Plant Associations of the Meadow Spittlebug, *Philaenus spumarius* (L.)." *PLoS One* 18, no. 10: e0291734. https://doi.org/10.1371/journal.pone.0291734.

Wang, J. J., Y. Ren, X. Q. Wei, and W. Dou. 2009. "Development, Survival, and Reproduction of the Psocid *Liposcelis paeta* (Psocoptera: Liposcelididae) as a Function of Temperature." *Journal of Economic Entomology* 102, no. 4: 1705–1713.

Weaver, C. R., and D. R. King. 1954. "Meadow Spittlebug *Philaenus leucophtalmus*." *Research Bulletin of the Ohio Agricultural Experiment Station* 741: 1–99.

Wells, J. M., B. C. Raju, H. Y. Hung, W. G. Weisburg, L. MandelcoPaul, and D. J. Brenner. 1987. "*Xylella fastidiosa* Gen. Nov., sp. Nov. Gram-Negative, Xylem-Limited, Fastidious Plant Bacteria Related to *Xanthomonas spp*." *International Journal of Systematic and Evolutionary Microbiology* 37: 136–143.

Whittaker, J. B. 1965. "The Biology of *Neophilaenus lineatus* (L.) and *N. exclamations* (Thunberg) (Homoptera: Cercopidae) on Pennine Moorland." *Proceedings of the Royal Entomological Society of London. Series A, General Entomology* 40, no. 4–6: 51–60.

Whittaker, J. B. 1973. "Density Regulation in a Population of *Philaenus spumarius* (L.) (Homoptera: Cercopidae)." *Journal of Animal Ecology* 42: 163–172.

Wiegert, R. G. 1964. "The Ingestion of Xylem Sap by Meadow Spittlebugs, *Philaenus spumarius* (L.)." *American Midland Naturalist* 71: 422–428.

Witsack, W. 1973. "Experimental and Ecological Investigations on Forms of Dormancy in Homoptera Cicadina Auchenorrhyncha Part 2 on Ovarian Parapause and Obligatory Embryonic Diapause in *Philaenus spumarius* Aphrophoridae." *Zoologischer Jahrbucher Systematic* 100: 517–562.

Yurtsever, S. 2000. "On the Polymorphic Meadow Spittlebug, *Philaenus spumarius* (L.) (Homoptera: Cercopidae)." *Turkish Journal of Zoology* 24, no. 4: 447–460.

Zajac, M. A., F. R. Hall, and M. C. Wilson. 1989. "Heat Unit Model for the Develppment of Meadow Spittlebug (Homoptera:Cercopidae) on Strawberry." *Environmental Entomology* 18: 347–350.

Zweig, M. H., and G. Campbell. 1993. "Receiver-Operating Characteristic (ROC) Plots: A Fundamental Evaluation Tool in Clinical Medicine." *Clinical Chemistry* 39: 561–577.

Supporting Information

Additional supporting information can be found online in the Supporting Information section. **Data S1:** Supporting Information.